Temporal changes of aeolian Saharan input in the Cape Verde abyssal plain since the last Glacial period

North Atlantic
Sediment
Post-glacial
Aeolian fluxes
Tracers

Atlantique Nord
Sédiment
Post-Glaciaire
Flux éoliens
Traceurs

Francis GROUSSET [a], Patrick BUAT-MENARD [b], Dominique BOUST [c], Ru-Cheng TIAN [a], Sophie BAUDEL [a], Claude PUJOL [a], Colette VERGNAUD-GRAZZINI [d]

[a] Unité Associée au CNRS n° 197, Université Bordeaux I, 351 Cours de la Libération, 33405 Talence Cedex, France.

[b] Centre des Faibles Radioactivités, Laboratoire Mixte CNRS-CEA, Domaine du CNRS, 91190 Gif-sur-Yvette, France.

[c] CEA-IPSN-DERS-SRTCM, Laboratoire de Radio-écologie Marine, B.P. 508, 50105 Cherbourg, France.

[d] Département de Géologie Dynamique, Université Paris VI, 4 place Jussieu, 75230 Paris, France.

Received 5/2/88, in revised form 3/8/88, accepted 15/9/88.

ABSTRACT

The mineralogical and geochemical study of a box-core recovered from the Cape Verde Abyssal Plain (Tropical North-East Atlantic) has been carried out to identify the African aeolian fingerprint, mainly in the 2-15 μm grain-size fraction. Together with mineralogical data, the Ti/Al ratio in this size fraction appears to be an excellent tracer of windborne particulate flux evolution. Our results indicate that aeolian fluxes have progressively decreased (by a factor of 7) since the last Glacial period, in relation with the post-Glacial warming. The Lower Holocene is identified as a low-wind transport period, with probable fluvial inputs, associated with the wet and warm climatic optimum. The Upper Holocene is marked by a re-activation of wind transport.

Oceanologica Acta, 1989. **11**, 2, 177-185.

RÉSUMÉ

Évolution des flux éoliens sahariens dans la plaine abyssale du Cap Vert, depuis la dernière période glaciaire

L'étude minéralogique et géochimique d'une carotte de type « boîte » prélevée dans la plaine abyssale du Cap Vert (Atlantique Nord-Est tropical) a été menée afin d'identifier l'empreinte éolienne africaine, principalement dans la fraction granulométrique typique des aérosols locaux (2-15 μm). Parallèlement aux traceurs minéralogiques, le rapport Ti/Al est un traceur fiable des flux éoliens particulaires. Les flux éoliens ont diminué progressivement d'un facteur 7, depuis la dernière période glaciaire, en relation avec le réchauffement post-glaciaire. L'Holocène inférieur est caractérisé par un affaiblissement des apports éoliens, et des apports fluviatiles faibles mais non négligeables. L'Holocène supérieur est marqué par une légère ré-activation des apports éoliens.

Oceanologica Acta, 1989. **11**, 2, 177-185.

INTRODUCTION

Aeolian input to oceanic sedimentation is today a well-established fact, but it is comprehensively documented only in oceanic areas at the latitude of major deserts: Gobi, Sahara, Australia (Chester *et al.*, 1979; Tetzlaff and Wolter, 1979; Prospero, 1981; Heath and Dymond, 1981; Sarnthein *et al.*, 1981-1982). The present-day extension of African aeolian dusts reaching the Atlantic Ocean has been particularly studied, and the origin of these particles has been determined by using mineralogical and geochemical criteria: the presence of quartz and clay minerals (Biscaye, 1965); Sr isotope ratios (Biscaye *et al.*, 1974; Grousset *et al.*, 1986); the abundance of elemental tracers such as Sc, Al, Th (Buat-

0399-1784/89/02 177 9/$ 2.90/© Gauthier-Villars

Menard and Chesselet, 1979). Close to Mauritania and Senegal, these aeolian components were clearly identified in margin sediments of the Atlantic Ocean by Sarnthein *et al.* (1982).

One unanswered question concerns the westward extension of this atmospheric input fingerprint in the sediment, since the last Glacial period. There is evidence that such a fingerprint can be found at distances greater than 1500 km from the African coasts. Indeed, it has been shown that quartz particles account for ≈5% of the surface sediment terrigenous fraction settling over the Mid Atlantic Ridge (MAR), close to 20°N (Beltagy *et al.*, 1972). This suggests that information on aeolian sediment deposition and atmospheric circulation may be obtained on the scale of the entire North Atlantic.

In this work, an attempt is made to determine paleo-aeolian flux variations in deep-sea sediments of the tropical North-East Atlantic Ocean, over the last 18,000 years B.P. For this purpose, we have selected a specific area, without any down-slope or bottom current transports (Jacobi and Hayes, 1981). In such an area, detrital sediments should be primarily derived from the aeolian contribution. Data presented here were obtained from the "Abyssal Plate" in the Cape Verde Abyssal Plain, where previous work suggested a major aeolian contribution to this area (Auffret *et al.*, 1984; Boust and Mauviel, 1985).

It is still possible, however, that in the past, river-derived inputs reached this region, either through down-slope processes (from the Senegal and other rivers) or from remote sources (Niger River), by intermediate water-mass advection. These rivers have drainage basins which are geographically distinct from areas eroded by both "Trade" and "African Easterly Jet" winds. Thus, it can be hypothetized that fluvial and aeolian signatures are geochemically different.

For the area studied, information is available concerning the present-day mineral dust input from the atmosphere. Two aerosol sampling cruises ("Gate" and "Midlante"), permitted the chemical characterization of the African aerosol input (Buat-Menard, 1979). However, calculated atmospheric fluxes during these cruises were shown to vary by one order of magnitude between two stations separated by only ≈600 miles of latitude. Because of their limited representativity, it is not possible to use such data to assess quantitatively the aeolian contribution to the Post-Glacial sedimentation in this region. Moreover, aeolian fluxes are submitted to short-period fluctuations (Savoie and Prospero, 1977), and may in the course of a single year, fluctuate by a factor of 30 (Prospero and Nees, 1977) from one week to another.

The only way to obtain the long-term trend is to study a sedimentary core, in which paleo-aerosol signals are integrated and short-term variations smoothed. We investigate with various techniques (grain-size, mineralogy, geochemistry) some specific aeolian parameters, and use them as paleo-input tracers. They include, for example, the Ti/Al ratio, already described by Boyle (1983) as a good aeolian tracer, or some elements which are enriched in Saharan dusts (Glaccum, 1978), such as: Cr, Cu, Ti, Sc or P.

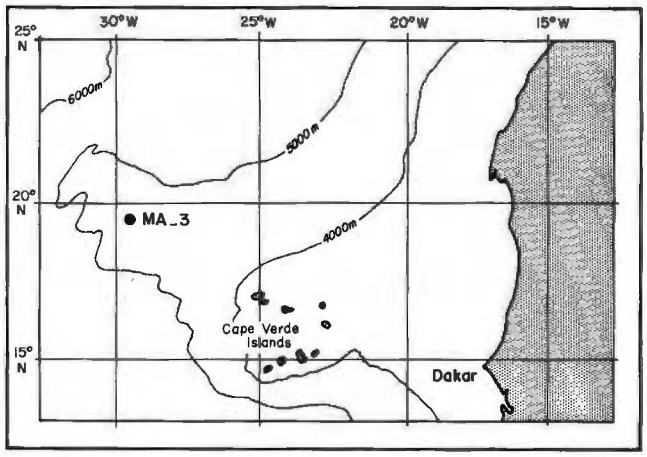

Figure 1
MA-3 core location.
Localisation de la carotte MA-3.

SAMPLING AND METHODOLOGY

Core MA-3 was sampled during the "Dialante" cruise, aboard the R/V "Marion Dufresne", in the position 19°24'N and 29°44'W, at a depth of 4910 m (Fig. 1). This core is located on the top of a small seamount, rising to about ≈300 m, above the surrounding Cape Verde abyssal plain. The area is located half-way between the continent and the MAR (≈1500 km from each). The distance from the continent restricts potential advective inputs, as confirmed by the low nepheloid layer context (Biscaye and Eittreim, 1976) and echo-facies patterns (Jacobi and Hayes, 1981; Sarnthein *et al.*, 1982). Moreover, this core is located in an area known to be quartz-enriched (Johnson, 1979), or rich in terrigenous silts ($\varnothing > 6\ \mu m$) (Sarnthein and Koopmann, 1980), interpreted as windborne components. According to Mauviel *et al.* (1982), ^{210}Pb measurements made in one neighboring core KG-40 (just 1 km distant), suggest that the mean bioturbation mixing depth is about 1 cm. Although this evaluation may be underestimated, it is nevertheless assumed that the sediments are not greatly disturbed and, consequently, that the paleo-aerosol imprint sequence must be preserved in the studied core.

Core MA3 was sampled with an undisturbing box-corer (interface-core sampler), which permits proper sampling of the first millimetre of the water/sediment interface (Veron *et al.*, 1987). The core length was about 32 cm, with a section of ≈7.5 × 10 cm. Layers 2 cm thick were sliced on board and stored at temperature of 4°C.

The following analyses were carried out:

– interstitial water content, gravimetrically measured before and after drying at 60°C;

– carbonate content ($\%CaCO_3$), measured with a gas-volumetric method;

– grain-size of the detrital fraction;

– mineralogical study (X-ray diffractometry) of major minerals (powder method) and of clay minerals (oriented-paste method);

– major element (Si, Al, Fe, Mn, Mg, Ti, K, P) and

trace element (Cu, Zn, Ni, Zr, Rb, S, Cr, Co, Nb) analyses were carried out by X-ray fluorescence, on bulk-dried and crushed samples. The biogenic silica contents were graphically-deduced from Si vs. Al plots. The detrital carbonate contents were graphically-deduced from $CaCO_3$ vs. total CaO plots. The oxidizing conditions which prevail in those sediments (Boust and Mauviel, 1985) allow us to consider that the chemical behaviour of some elements (Ti, Al, *etc.*) is not affected by diagenesis. Such elements may thus be considered as source tracers.

Lastly, we analyzed the same elements in six different grain-size fractions (0-2 μm, 2-6 μm, 6-10 μm, 10-15 μm, 15-63 μm and ≧ 63 μm) after a gentle 0.1 N-HCl-leaching of the carbonate content. We checked with a microprobe that this attack was gentle enough to avoid any clay mineral deterioration. These grain-size fractions were broken up by sieving and decantation, followed by a Sedigraph Coultronics Analyzer control (Baudel, 1985).

– The study of planktonic foraminifera species (method in Pujol (1980)), and $\partial^{18}O$ and $\partial^{13}C$ measurements on *G. Trilobus*, gives us a preliminary stratigraphic scale. From these data, it was then possible to evaluate carbonate-free fraction sedimentation rates. For a given period, fluxes (in $g.cm^{-2}.ky^{-1}$) are calculated from the corresponding sediment thickness, the pore-water content, and by assuming a mean density for the terrigenous particles of about $\approx 2.65\ g.cm^{-3}$.

RESULT

The sediment is very homogeneous, and consists of a fine-grained brown ooze, mainly composed of planktonic foraminifera and calcareous nannoflora. We did not observe any structure. The terrigenous silty fraction ($\varnothing = 2\ \mu m - 63\ \mu m$) does not exceed ≈6% and the terrigenous sand fraction ($\varnothing > 63\ \mu m$) was found to be negligible.

• *The biostratigraphic analysis of planktonic foraminifera* led us to distinguish three different units, boundaries of which are inferred from $\partial^{18}O/^{16}O$ data (Fig. 2):

– the level 15,000 yrs B.P. is located close to the core bottom (≈ -30 cm); the "termination IA" (13,000 yrs B.P.; after Pujol, 1980) could be located around ≈ -28 cm; and the "Termination IB" (9,000 yrs B.P.) close to ≈ -10 cm. According to these three dated events, it is possible to propose the following main stratigraphic unit ages:

– the "Late Glacial" period (15,000 to ≈11,000 yrs B.P.): *unit A*. In this area, we know that Globorotalia Menardii appeared close to ≈11,000 yrs. B.P. (Pujol, 1980);

– the "Lower Holocene" (≈11,000 to ≈6,000 yrs B.P.): *unit B*. Tropical planktonic species reach their largest amount for this period;

– the "Upper Holocene" (≈6,000 yrs B.P.-today): unit C.

It is thus possible to evaluate the mean accumulation rate: $\approx 1\ cm.ky^{-1}$, for the entire Holocene period. This value is in good agreement with previous evaluations proposed for this region: $0.93\ cm.ky^{-1}$ (Peterson *et al.*, 1972) or $0.9\ cm.ky^{-1}$ (Mauviel *et al.*, 1982). The Late Glacial accumulation rate (unit A) is four times the Holocene one: $\approx 4.5\ cm.ky^{-1}$.

Table 1

Mineralogy of the clay-size ($\varnothing < 2\ \mu m$) detrital fraction (S = smectite, K = kaolinite, C = chlorite, I = illite, A = attapulgite).

Minéralogie de la fraction détritique argileuse ($\varnothing < 2\ \mu m$) (S = smectite, K = kaolinite, C = chlorite, I = illite, A = attapulgite).

Levels (cm)	Kaolinite (%)	Illite (%)	Smectite (%)	Chlorite (%)	Attapulgite (%)
0	41	20	20	11	8
1	39	24	18	9	9
3	40	22	19	11	8
5	41	24	18	10	9
7	40	25	19	10	7
9	40	23	22	9	6
11	44	22	20	9	6
13	49	19	21	7	5
15	56	17	16	7	5
17	43	20	23	9	6
19	47	23	14	11	5
21	45	23	17	10	5
23	46	23	14	12	5
25	44	24	16	12	5
27	40	22	21	11	5
29	38	25	22	9	6
31	37	22	26	12	3

• *Main minerals* are : carbonate (58-81%), clay minerals (16-38%) and quartz (3-9%). Allochtonous detrital carbonates account for less than 4% of the bulk sediment (Tian, 1984). The small biogenic opal content – diatoms and radiolarians – decreases from 3.6% (unit A) down to 0.8% (unit C). Clay minerals are: kaolinite (37-56%), illite (17-25%), smectite (14-26%) and chlorite (7-12%; Tab. 1). Palygorskite (attapulgite) seems to be a minor mineral (3-9%). Whereas units A and C have a quite similar mineralogical composition, unit B is comparatively poorer in illite (and poorer

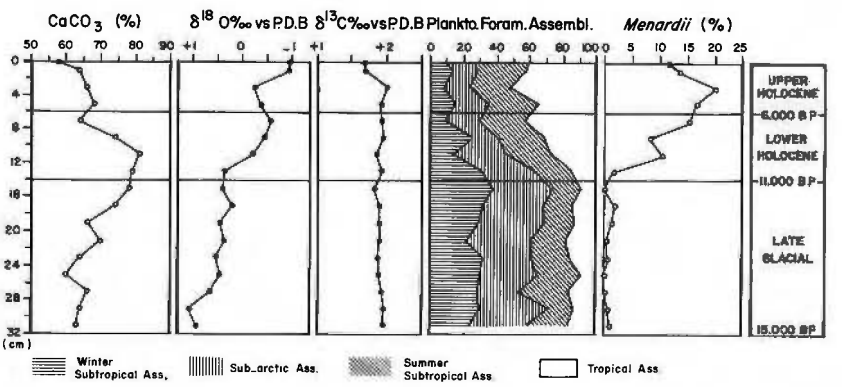

Figure 2

Planktonic foraminifera: distribution, $\partial^{18}O$ and $\partial^{13}C$ analyses and stratigraphic interpretation.

Foraminifères planctoniques : distribution, courbes isotopiques ($\partial^{18}O$ et $\partial^{13}C$) et interprétation stratigraphique.

Table 2
Major element concentrations (%) in every 2 cm core segment of bulk sediment.
Évolution verticale des teneurs pondérales de quelques éléments majeurs dans le sédiment total (%).

Levels (cm)	Si (%)	Al (%)	Fe (%)	Mn (%)	Mg (%)	Ti (%)	K (%)	P (%)	Ti/Al
0	22.5	7.5	3.4	0.092	4.28	0.26	0.17	0.21	0.035
1	21.9	7.2	3.6	0.1	4.49	0.28	0.18	0.22	0.039
3	24	8.1	3.6	0.1	4.9	0.28	0.17	0.24	0.035
5	22.4	7.7	3.3	0.092	5.38	0.24	0.1	0.23	0.031
7	30.3	8.5	3.75	0.1	6.19	0.27	0.13	0.32	0.032
9	28.9	9.8	3.9	0.123	7.6	0.27	0.04	0.405	0.028
11	30.5	9.5	4.2	0.131	7.29	0.31	0.08	0.4	0.033
13	27.6	9.1	3.7	0.115	6.14	0.28	0.17	0.475	0.031
15	24.3	7.6	3.6	0.108	4.52	0.29	0.37	0.26	0.038
17	25.1	9	4.3	0.123	4.72	0.36	0.415	0.2	0.040
19	25.2	9.2	4.55	0.146	4.2	0.38	0.48	0.21	0.041
21	26.7	8.5	4.1	0.131	4.66	0.33	0.35	0.24	0.039
23	25.7	7.8	3.8	0.123	4.15	0.31	0.35	0.23	0.040
25	23	8.6	3.55	0.123	4.42	0.29	0.34	0.22	0.034
27	27.9	9.5	4.3	0.154	4.88	0.35	0.42	0.22	0.037
29	24.3	8.9	4.1	0.139	2.84	0.33	0.41	0.27	0.037
31	27	9.7	5	0.162	4.57	0.41	0.58	0.2	0.042

Table 3
Trace element concentrations ($\mu g.g^{-1}$) in every 2 cm core segment of bulk sediment.
Évolution verticale des teneurs pondérales de quelques éléments traces dans le sédiment total ($\mu g.g^{-1}$).

Levels (cm)	Nb	Cu	Zn	Ni	Zr	Rb	Cr
0	81	190	105	53	130	176	58
1	62	198	105	73	136	193	46
3	58	205	107	70	154	202	66
5	69	209	89	65	138	205	66
7	75	269	104	72	162	242	62
9	115	323	109	90	200	269	54
11	94	352	144	99	196	282	55
13	82	252	121	74	186	239	46
15	70	213	105	105	164	191	56
17	69	204	111	181	185	194	59
19	70	192	114	91	190	200	73
21	72	211	122	82	180	207	61
23	61	196	118	97	174	191	53
25	66	180	109	76	154	157	53
27	71	215	123	91	176	218	49
29	65	203	108	81	168	183	68
31	62	234	121	109	191	218	69

still in chlorite) and richer in kaolinite; however, this anomaly is slightly shifted downcore, starting before the end of unit A. Lastly, smectite and kaolinite are mostly located in fine fractions, and illite is more abundant in the silty fraction.

- *Major elements* are nearly constant over the entire core length (Tab. 2). However, their relative proportions differ from one period to another. This is the case of Ti/Al and Si/Al. Some enrichments are also observed in unit B: $\approx +25\%$ for Si, or $\approx +100\%$ for P. Moreover, Si, K and Ti are more abundant in the 2-15 μm grain-size fraction.

- *Trace elements* display too little variability (Tab. 3), except perhaps for Rb, Nb and Cu—which appear enriched during unit B if they are expressed on a carbonate-free basis. Chemical analyses performed on the decarbonated grain-size fractions (Tab. 4), indicate that Al, Fe and Th are more abundant in the clay-size fraction, Cs in the 2-6 μm fraction (unit B), Ti in the 10-15 μm fraction, and Si, K, Ti, Rb, Cu, Zr, Nb, and Th in the 2-15 μm grain-size fraction. In the discussion, we shall exclude some labile elements such as Fe, Mn, K, which seem to be enriched in the bottom core and cannot therefore be used as source tracers (Boust *et al.*, 1988).

- $^{87}Sr/^{86}Sr$ ratio measured in the detrital (carbonate-free) fraction of the top centimetre of the core, is about 0.72125 (Grousset *et al.*, 1986).

- *Terrigenous* (Φ_t) *and biogenic* (Φ_b) *fluxes* (Tab. 5): Terrigenous fluxes are approximately $\approx 1.75\ g.cm^{-2}.ky^{-1}$ during unit A; they decrease down to $0.45\ g.cm^{-2}.ky^{-1}$ during unit B, and do not exceed $0.26\ g.cm^{-2}.ky^{-1}$ during unit C. Since the Late Glacial period, these fluxes have therefore decreased by a factor of 7. Carbonate fluxes decrease in the same way (from $\approx 3\ g.cm^{-2}.ky^{-1}$ down to $\approx 0.45\ g.cm^{-2}.ky^{-1}$), except for unit B, where Φ_t/Φ_b is almost twice as low as during the two other periods.

DISCUSSION

From these data, a series of questions arise: Why have fluxes decreased since the Last Glacial maximum? why are units A and C quite similar and why is unit B different from the other two? Is there an alternation in particle sources, in transport mechanisms (wind, river, currents), or an aeolian input weakening? In the following discussion, flux evolution as well as geochemical

and mineralogical criteria will be used to explain temporal patterns observed.

Hypothesis on flux temporal evolution

Is it possible to evaluate the aeolian flux evolution from the detrital flux values? Detrital flux values (Tab. 5) display a decreasing trend since the last Glacial period. This terrigenous flux decrease may be explained by two different processes:

- *First hypothesis: the flux decrease is mainly induced by a diminishing shelf (and fluvial) input.* In this case, we have to assume that the inputs reached the studied area via down-slope processes, and were not determined by surface water primary productivity. Indeed, such down-slope processes took place along the margin: Sarnthein and Diester-Hass (1977) determined that during the Last Glacial maximum, Senegal slopes were fed by aeolian silty and sandy turbidites, originating on the outershelf. Close to 18,000 yrs B.P., this boundary was the shoreline and aeolian sand dunes were built along the shelf. This process may explain why the unit A flux is seven times larger than that of unit C (Tab. 5). On the other hand, rivers were active during unit B: climate was much wetter than today and the Senegal River detrital output was certainly higher (Sarnthein *et al.*, 1981). Thus, the continent at that latitude was probably covered by more vegetation, which is a limiting factor for aeolian erosion.

But in none of the three units do we observe any turbiditic or current transport-derived structure which could have been induced by similar advective inputs. This implies that only the distal extremity of turbidity currents could have reached the studied area: such particles have too small a grain-size ($\varnothing < 10\ \mu m$) to

Table 4

Major (%) and trace element ($\mu g.g^{-1}$) contents in five decarbonated grain size fractions (0-2 µm, 2-6 µm, 6-10 µm, 10-15 µm, 15-63 µm). Analyses were carried out on three different core sections corresponding to the three units.

Teneurs en éléments majeurs (%) et traces ($\mu g.g^{-1}$) dans cinq fractions granulométriques décarbonatées de la phase terrigène (0-2 µm, 2-6 µm, 6-10 µm, 10-15 µm, 15-63 µm); les analyses ont été réalisées sur les trois segments de carotte correspondant aux trois unités.

	Si (%)	Al (%)	Fe (%)	Mn (%)	Mg (%)	Ti (%)	K (%)	P (%)
Unit C:								
0-2 µm	23.6	10.4	7.6	0.048	1.58	0.74	2.47	0.092
2-6 µm	26.9	9.7	5.7	0.046	1.61	0.8	2.51	0.07
6-10 µm	31.6	7.2	4.6	0.042	1.02	0.83	2.2	0.066
10-15 µm	34.4	5.9	3.8	0.046	0.64	0.85	1.87	0.07
15-63 µm	33	6.5	4	0.043	1.05	0.51	1.88	0.062
Unit B:								
0-2 µm	22.2	11.4	8.2	0.044	1.97	0.77	2.51	0.092
2-6 µm	26.8	9.6	6.3	0.043	1.49	0.84	2.56	0.07
6-10 µm	32.2	7	4.4	0.044	1.03	0.77	2.03	0.066
10-15 µm	35.1	5.3	3.9	0.054	0.55	0.93	1.72	0.066
15-63 µm	32.9	6.5	4.2	0.041	1.24	0.46	2.03	0.066
Unit A:								
0-2 µm	22.7	11.2	8.4	0.049	1.51	0.83	2.42	0.084
2-6 µm	28.1	9.1	5.6	0.05	1.36	0.76	2.27	0.07
6-10 µm	32.4	6.9	4.5	0.049	0.8	0.77	2.11	0.07
10-15 µm	34.9	5.4	4.1	0.059	0.55	0.86	1.75	0.066
15-63 µm	33.3	7.3	3.5	0.035	0.85	0.53	1.82	0.066

	Nb (ppm)	Cu (ppm)	Ba (ppm)	Zn (ppm)	Ni (ppm)	Zr (ppm)	S (ppm)	Cs (ppm)	Ca (ppm)	Cr (ppm)	Rb (ppm)
Unit C:											
0-2 µm	49	109	393	124	58	107	721	1.4	5.3	112	163
2-6 µm	47	100	629	113	62	117	528	0.1	6.5	96	156
6-10 µm	52	96	555	96	47	177	331	4.6	6	65	148
10-15 µm	56	90	462	76	34	331	315	0.1	11.4	67	127
15-63 µm	36	93	502	85	32	109	263	8.2	1.1	49	144
Unit B:											
0-2 µm	52	124	578	128	65	111	711	0.1	14.8	116	164
2-6 µm	56	105	819	118	60	120	551	12.3	12.4	106	167
6-10 µm	56	101	728	97	45	176	394	5.4	4.3	66	140
10-15 µm	60	92	536	67	34	381	356	7.2	0.1	74	121
15-63 µm	37	103	534	85	41	139	312	0.1	0.1	48	146
Unit A:											
0-2 µm	58	118	909	116	59	117	727	0.1	12.3	104	158
2-6 µm	50	142	1246	119	57	126	571	3.9	3.8	77	160
6-10 µm	49	92	832	88	41	169	403	0.1	10.2	63	136
10-15 µm	52	86	732	69	30	338	320	3.2	4.1	61	124
15-63 µm	31	90	542	69	34	150	297	0.1	5	49	120

Table 5

Terrigenous ($\varnothing_t$) and biogenic carbonate ($\varnothing_b$) fluxes for the three main units. Fluxes are derived from water-content-free accumulation rates, and expressed in $g.cm^{-2}.10^3\ yrs^{-1}$.

Flux terrigènes (0_t) et flux biogènes carbonatés (0_b) dans les trois unités majeures (les flux sont calculés à partir des taux de sédimentation corrigés de la teneur en eau, et sont exprimés en $g.cm^{-2}.10^3\ yrs^{-1}$).

Units	Terrigenous Fluxes ($\varnothing_t$)	Biogenic Fluxes ($\varnothing_b$)	$\varnothing_t/\varnothing_b$
C	0.26	0.45	0,578
B	0.45	1.25	0,360
A	1.75	3.00	0,583

be able to build any structure. In any case, down-slope inputs could alone explain the detrital flux evolution. Unit B only may have been concerned by a slight fluvial component, but we cannot evaluate the fluvial/aeolian detrital flux proportions.

• *Second hypothesis: the main transport mechanism for detrital particles was wind transport, even* 1,500 *km off continental coasts.* At least for unit C, a windborne signature is confirmed by isotopic tracers: the $^{87}Sr/^{86}Sr$ ratio measured in the carbonate-free fraction of the top centimetre of the core ($\approx$0.72125), is consistent with the Saharan aerosol isotopic signature: $\approx$0.717/$\approx$0.721 (Biscaye *et al.*, 1974), and very different from the present-day Senegal River sediment value: 0.72858 (Biscaye *et al.*, in prep.). Consistent results were obtained with neodymium isotopes (Grousset *et al.*, 1988).

In this hypothesis, aeolian particles have to pass through surface watermasses where biological primary productivity takes place. As the primary productivity is relatively high in this area: $\approx 60\ mg.C.m^{-2}.day^{-1}$ (Berger *et al.*, 1986), these particles are immediatly incorporated into large particles – fecal pellets and bioaggregates (Honjo, 1982). The residence time of large particles is certainly short (Bruland and Coale, 1986). This rapid sinking is a limiting factor for potential watermass re-advection and scattering. Then, we may assume that sedimentary flux patterns reflect faithfully aerosol patterns and that the Φ_t evolution is mainly controlled by primary productivity evolution. Thus, the observed flux decrease should be induced by a windborne particle flux decrease. This is supported by data reported eastward by Muller and Suess (1979): productivity decreased progressively from the Last Glacial period ($\approx 200\ g.C.m^{-2}.yr^{-1}$), throughout the lower Holocene ($\approx 150\ g.C.m^{-2}.yr^{-1}$), and down to $\approx 75\ g.C.m^{-2}.yr^{-1}$, today. This is also consistent with the $CaCO_3$ flux evolution (Tab. 5): this biogenic flux decreased from $\approx 3\ g.cm^{-2}.ky^{-1}$ during the late Glacial, down to $0.45\ g.cm^{-2}.ky^{-1}$ during the Upper Holocene. The possibility of a $CaCO_3$ dissolution is rejected: Boust and Mauviel (1985) demonstrated that this process is extremely weak in this area.

Now, we have to understand why we observe such a terrigenous flux depletion in unit B, compared to unit A. We must assume that wind transport decreased strongly during unit B (lower Holocene), 1,500 km off the Senegal coast. This is probably a remote echo of the slowing down of the "African Easterly Jet" wind regime which occurred during this period. On the basis of a pollen analysis, Rossignol and Duzer (1979) have already reported the existence of such an event close to the Senegal coast, between $\approx$12,000 and $\approx$5,500 yrs B.P. Moreover, African "Melosira" (lacustrine diatoms) were studied in a neighbouring (18°N-21°W) core: V30-49 (Pokras and Mix, 1985). These authors report a similar abundance curve, displaying depletion during unit B. These diatoms are mainly transported by wind from Africa (Folger, 1970). Their size is smaller than $\approx 20\ \mu m$: this is consistent with the detrital particle size range that we found in core MA-3. Thus, biological tracer evolutions are in agreement with mineralogical and geochemical information and would reflect the paleo-aeolian input fluctuation since the last Glacial period.

Now, in order to choose between these two hypotheses, we have to take into consideration information provided by both mineralogical and geochemical parameters.

Information provided by mineralogical parameters

In Saharan dusts settling today over the Cape Verde Basin, the main minerals are kaolinite ($\approx$25%), illite ($\approx$22%) and smectite ($\approx$19%) (Prospero *et al.*, 1970; Glaccum, 1978). Illite is abundant in the "Trade" dusts and kaolinite and smectite are the main components of the "African Easterly Jet" aerosols (Prospero, 1981; Sarnthein *et al.*, 1981). In the sediment, we found these minerals in the same proportions (Tab. 1), except for kaolinite, which is too abundant ($\approx$44%) compared to present-day aerosol data, mainly during unit B. On the time-scale covered by this study, we may exclude the possible effect of diagenesis on the clay minerals and consider them as "quasi-conservative" tracers (Biscaye, 1965). We may explain this excess by a wind trajectory shift, inducing aerosol deflation over a different source area. But it is still possible that a slight complementary advective input came from African rivers: *e.g.* the Senegal River, in where the kaolinite content is today about 39% (Gac and Kane, 1986). Some authors even suggested a possible Niger River contribution (Biscaye, 1965; Lange, 1982).

Finally, we used the graphic-method from Windom (1969), which involves deducing the aeolian contribution through the present-day aerosol mineralogy and sediment mineralogical composition. Here, the authigenic attapulgite (Bonté *et al.*, 1980; Tian, 1984) is considered as the non-aeolian parameter. We obtain the following evaluation: $\approx$80% of the carbonate-free fraction would be transported by wind during units A and C, but only $\approx$60% during unit B. These results are consistent with the interpretation proposed above.

Information provided by geochemical tracers

First, we have attempted to recognize, in the sediment, some specific aeolian geochemical tracers. These tracers were sought mainly in the same grain-size range as in the Saharan aerosol.

The mean grain-size of the aerosol settling over Cape Verde Islands is about $\approx$10-20 μm, and decreases to $\approx$2-4 μm over the MAR (Gac et Travi, 1984). Our core is located between these two areas: thus, the grain size fraction which must contain the major aeolian contribution ranges between $\approx 2\ \mu m$ and $\approx 15\ \mu m$. This is much coarser than the local fluvial contribution: indeed, $\approx$90% of the present-day Senegal River particles are smaller than 2 μm (Gac and Kane, 1986). Moreover, in terms of fluxes, the present-day Saharan aeolian flux is about 70.10^6 tons/year (Gannor and Maname, 1982), when the Senegal River suspended matter flux is currently about 2.10^6 tons/year (Gac and Kane, 1986). Thus, most of the 2 to 15 μm particles are in all likelihood windborne.

In core MA3, the Ti/Al ratio reaches its maximum value in the 6-15 μm fraction (up to ≈0.17). This size range is very similar to the present-day aerosol grain-size range over this region. In these aerosols, Ti/Al reach values as high as 0.07 (after Prospero, 1981). High during unit A (0.038+/−0.001), the Ti/Al ratio decreased during unit B (0.031+/−0.001) and rose again during unit C (0.035+/−0.002; Fig. 3). Ti/Al ratios in units A and C are very similar to the tropical aerosol ratio: 0.073 (Ti and Al values from Prospero, 1981). We must refer to the African lacustrine diatom abundance curves reported by Pokras and Mix (1985) in the Tropical North-East Atlantic, which are extremely similar to our Ti/Al curve. This is an independent parameter which supports the aeolian significance that we claim for the Ti/Al ratio. Moreover, this evolution is also observed with other ratios: Nb/Al or Cu/Al (Fig. 3). For this last ratio (Cu/Al), for example, units C and A display "high" values ($\approx 10.10^{-4}$) similar to aerosol ratios: $\approx 14.5.10^{-4}$ (after Prospero, 1981); conversely, unit B displays "low" values ($\approx 6.5.10^{-4}$) close to the present-day suspended particulate matter of the Senegal River: $\approx 4.10^{-4}$ (after Gac and Kane, 1986). This event cannot be explained by diagenetic processes: there is no typical redox anomaly at that depth (Tian, 1984; Boust and Mauviel, 1985).

As reported by Glaccum (1978) in Saharan dusts, Ti, Cr, Cu, Sc and P are enriched in the ≈2-15 μm fraction. Moreover, this author reports a Si/Al ratio equal to ≈2.95, and we find in the sediment, values from ≈2.7 to 3.5 (Tab. 2), while this ratio is only about 1.86 in the Senegal River (after Gac and Kane, 1986). On the other hand, we observe a negative correlation between Ti/Al and Si/Al. Obviously, biogenic silica is excluded in this comparison. Si appears to be associated with the fine grain-sized fraction, preferentially carried out by rivers: here, perhaps, the Senegal River (Sarnthein *et al.*, 1981). Among the only elements in the aerosols with soil-like enrichment factors is Ti, when elements with rock-like enrichment factors include Si (Rahn, 1976). Thus, Ti tends to characterize the aeolian input inherited from a petrographically more "basaltic" province, enriched in Ti-rich soil minerals (ilmenite) and located in the central and southern part of Sahara, compared to more "acidic" rocks which are drained by rivers in the western part of Sahara.

Together with this explanation, it is still possible that, during unit C, the African lateric soil pattern shifted latitudinaly, inducing a slight change in the aerosol geochemical signature. At the same time, the vegetal cover spread northwards, probably inibiting the aeolian deflation. Further investigation on the continent will be necessary to clarify this matter.

For these numerous reasons, we prefer the second of the hypotheses proposed above. Thus, we propose that aeolian fluxes were really high during unit A (seven times the present-day value). On one hand, this discrepancy was predicted by theoretical models (Joussaume, 1983); on the other, Petit *et al.* (1981) reported that Glacial aeolian fluxes in the South Pole

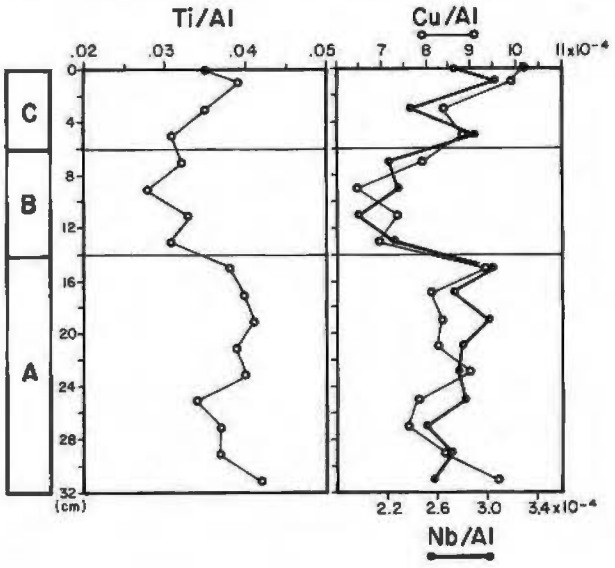

Figure 3
Ti/Al, Cu/Al and Nb/Al ratios: down-core evolutions.
Évolution verticale des rapports pondéraux : Ti/Al, Cu/Al et Nb/Al.

ice-cap were 10 times greater than today, and Thompson and Mosley-Thompson (1981) reported an enrichment factor of 12 in the Greenland ice-cap. Conversely, B unit corresponds to a highly wet event – the climatic optimum –, occurring shortly after the extremely dry Glacial maximum period (Sarnthein *et al.*, 1981). Moreover, pollen analysis of some Senegal shelf and slope cores allowed Rossignol and Duzer (1979), to identify a strong decrease in aeolian fluxes, and a Senegal river input enhancement. In the same way, Pokras and Mix (1985) observed a strong windborne lacustrine diatom decrease in core V30-49, induced by a rising African lake level. We observe the same evolution in a more remote part of the Ocean.

CONCLUSION

- 1500 km from the African continent, deep sediments of the Cape Verde abyssal plain received windborne particles emitted by the Saharan desert area. The geochemical signature of this aeolian input has been recognized in sediments, mainly in the grain-size range corresponding to that of the present-day regional aerosol (≈2 μm-15 μm). The Ti/Al ratio can be used as an aeolian input index. In this regime, it was not possible to distinguish any aeolian fluctuation with only lithology, structure, facies or other classical observations.

- We recognized three main periods:

– the Late Glacial period (≈15,000-≈11,000 yrs B.P.) characterized by an aeolian flux which was 7 times the present-day flux. As suggested eastward by Diester-Hass (1976), atmospheric input may explain entirely the unit A detrital flux;

– the Lower Holocene (≈11,000-≈6,000 yrs B.P.), during which the aeolian input decreased, while a fluvial component occurred;

– the Upper Holocene (≈6,000-≈today), marked by a wind transport activation, without any riverine input. The Upper Holocene detrital flux was about ≈260 mg.cm^{-2}.ky^{-1}. This is consistent with present-day aeolian fluxes, which are situated within a range of ≈140 and 700 mg.cm^{-2}.ky^{-1} (Ku *et al.*, 1968).

• The paleo-aerosol imprint memorized in such a remote abyssal plain has only a latitudinal significance, and cannot be extended to the entire Ocean. For instance, during the Lower Holocene, we observed that wind transport over the Atlantic Ocean was weak at the trade latitudes (≈10°-30°N), whereas in the westerlies (≈40°-60°N), it was enhanced both in the North Atlantic (Grousset and Chesselet, 1986) and in the North Pacific (Janecek and Rea, 1986).

Acknowledgements

We are grateful to Drs. Claude Lambert and Claude Latouche for their reviews of an early draft of the manuscript, and to Pr. Michael Sarnthein who helped us with critical discussions. We thank Pr. Roy Chester and two anonymous reviewers for their comments. $\partial^{13}C$ and $\partial^{18}O$ ratios were analyzed by one of the authors (C. V.-G.) in the *Département de Géologie Dynamique* (University Paris VI). The MA-3 core was recovered during the "Dialante" cruise: we are most grateful to the officers and crew of the R/V Marion-Dufresne. This cruise was funded by the *Commissariat à l'Énergie Atomique* (CEA), by the *Territoires et Terres Australes et Antarctiques Françaises* (TAAF) and by the *Centre National de la Recherche Scientifique* (*CNRS*).

REFERENCES

Auffret G. A., R. Le Suave, B. Sichler, R. Kerbrat, S. Roy, C. Laj, C. Muller, C. Maillet and C. Latouche (1984). Sédiments tertiaires et quaternaires du plateau abyssal du Cap-Vert. *Bull. Soc. géol. Fr.*, **7**, 261, 33-45.

Baudel S. (1985). L'apport éolien dans la sédimentation océanique : synthèse bibliographique (application à l'étude de la plaine abyssale du Cap Vert). *Mémoire D.E.A., Université Bordeaux I*, 61 pp.

Beltagy A. I., R. Chester and R. C. Padgham (1972). The particle size distribution of quartz in some North Atlantic deep-sea sediments. *Mar. Geol.*, **13**, 297-310.

Berger W. H., K. Fischer, C. Lai and G. Wu (1986). Primary production and organic carbon flux in the world ocean. *AGU abstract, New-Orleans, January* 1986.

Biscaye P. E. (1965). Mineralogy and sedimentation of recent deep-sea-clay in the Atlantic Ocean and Adjacent Sea and Oceans. *Geol. Soc. Am. Bull.*, **76**, 803-832.

Biscaye P. E. and C. E. Eittreim (1977). Suspended particulate loads in the nepheloid layer of the Abyssal Atlantic Ocean. *Mar. Geol.*, **22**, 155-172.

Biscaye P. E., R. Chesselet and J. Prospero (1974). Rb-Sr, $^{87}Sr/^{86}Sr$ isotope system as an index of provenance of continental dusts in the open Atlantic Ocean. *J. Rech. atmos.*, **8**, 3/4, 819-829.

Biscaye P. E., F. E. Grousset and J. Dasch (in prep.). Rubidium-Strontium "model age" in deep-sea sediments and aerosols: Atlantic Ocean.

Bonté P., C. Lalou and C. Latouche (1980). Ferromanganese deposits in cores from the Kane and Atlantic fracture areas: possible relationships with hydrothermalism. *J. Geol. Soc.*, **134**, 373-377.

Boust D. and A. Mauviel (1985). Sedimentological and geochemical investigation of an abyssal oligotrophic environment on the Cape Verde abyssal plain (North Atlantic Ocean). *Oceanologica Acta*, **8**, 2, 157-165.

Boust D., M. S. N. Carpenter and J.-L. Joron (1988). Investigation of authigenic and diagenetic processes by chemical leaching of pelagic sediments from the Cape Verde abyssal plain. *Chem. Geol.*, **68**, 69-87.

Boyle E. A. (1983). Chemical accumulation variations under the Peru current during the past 130,000 years. *J. geophys. Res.*, **88** C12, 7667-7680.

Bruland K. W. and K. H. Coale (1986). Surface water $^{234}Th/^{238}U$ desequilibria: a tracer of spatial and temporal variations of scavenging rates. In: *Dynamic processes in the chemistry of upper ocean*, J. D. Burton, P. G. Brewer and R. Chesselet, editors, NATO Advanced Research Institute, Jouy-en-Josas, 1983, Plenum Press, England.

Buat-Menard P. (1979). Influence de la retombée atmosphérique sur la chimie des métaux en trace dans la matière en suspension de l'Atlantique Nord. *Thèse Doctorat ès Sciences, University Paris*, pp. 434.

Buat-Menard P. and R. Chesselet (1979). Variable influence of the atmospheric flux on the trace metal chemistry of oceanic suspended matter. *Earth planet. Sci. Letts*, **42**, 399-411.

Chester R., A. G. Griffiths and J. M. Hirst (1979). The influence of soil-sized atmospheric particulates on the elemental chemistry of the deep-sea sediments of the northeastern Atlantic. *Mar. Geol.*, **32**, 141-154.

Diester-Hass L. (1976). Late Quaternary climatic variations in Northwest Africa deduced from East Atlantic sediment cores. *Quat. Res.*, **6**, 299-314.

Folger D. W. (1970). Wind-transport of land-derived mineral biogenic and industrial matter over the North Atlantic. *Deep-Sea Res.*, **17**, 337-352.

Gac J.-Y. and Y. Travi (1984). Étude quantitative des poussières atmosphériques en provenance du Sahara, entre Dakar et Nouakchott. 10^{e} *RAST, Bordeaux*, pp. 237.

Gac J.-Y. and A. Kane (1986). Le Fleuve Sénégal : I. Bilan hydrologique et flux continentaux de matières particulaires à l'embouchure. *Sci. Géol. Bull.*, **39**, 1, 99-130.

Gannor E. and Y. Maname (1982). Transport of Saharan dust across the Eastern Mediterranean. *Atmos. Environ.*, **16**, 3, 581-587.

Glaccum R. A. (1978). The mineralogical and elemental composition of mineral aerosols over the tropical North Atlantic: the influence of Saharan dust. *Thesis, University Miami, Florida*, 160 pp.

Grousset F. E. and R. Chesselet (1986). The Holocene sedimentary regime in the Northern Mid-Atlantic Ridge Region. *Earth planet. Sci. Letts.*, **78**, 271-287.

Grousset F. E., P. E. Biscaye and A. Zindler (1986). Nd and Sr isotopes in North-East Atlantic detrital particles, *Eos*, **67**, 44, 900.

Grousset F., P. E. Biscaye, A. Zindler, J. Prospero and R. Chester (1988). Neodymium isotopes as tracers in marine sediments and aerosols: North Atlantic. *Earth planet. Sci. Letts.*, **87**, 367-378.

Heath G. R. and J. Dymond (1981). Metalliferous sediment deposition in time and space: East Pacific Rise and Bauer Basin, northern Nazca Plate. *Geol. Soc. Am. Mem.*, **154**, 175-198.

Honjo S. (1982). Seasonality and interaction of biogenic and lithogenic particulate flux at the Panama Basin. *Science*, **218**, 883-884.

Jacobi R. D. and D. E. Hayes (1981). Bathymetry, microphysiography and reflectivity characteristics of the west African continental margin: Sierra Leone to Mauritania. In: *Geology of West African continental margin*, Von Rad *et al.*, editor, Springer-Verlag, Heidelberg, 182-212.

Janecek T. R. and D. K. Rea (1986). Quaternary fluctuations in the Northern hemisphere tradewinds and westerlies. *Quat. Res.*, **24**, 150-163.

Johnson L. R. (1979). Mineralogical dispersal patterns of the North Atlantic deep-sea sediment with particular reference to aeolian dusts. *Mar. Geol.*, **29**, 335-345.

Joussaume S. (1983). Modélisation des cycles des espèces isotopiques de l'eau et des aérosols d'origine désertique dans un modèle de circulation général de l'atmosphère. *Thèse 3e Cycle, Université Paris VI*, 202 pp.

Ku T. L., W. S. Broecker and N. Opdyke (1968). Comparison of sedimentation rates measured by paleomagnetic and ionium methods of age determination. *Earth planet. Sci. Letts*, **4**, 1-16.

Lange H. (1982). Distribution of chlorite and kaolinite in eastern Atlantic sediments, off North Africa. *Sedimentology*, **29**, 427-431.

Mauviel A., H. V. Nguyen, R. Chesselet, M. Sibuet, Y. Yokoyama and G. Auffret (1982). Étude des variations des taux de bioturbation par la spectrométrie gamma non destructive (GeHP), dans trois zônes sédimentaires de l'Atlantique Nord, à 200 m, et à plus de 4000 m de profondeur. Coll. Interna. CNRS, Bordeaux 22/25-09-81, *Bull. IGBA*, **31**, 257-274.

Muller P. J. and E. Suess (1979). Productivity, sedimentation rate and sedimentary organic matter in the oceans. 1: Organic carbon preservation. *Deep-Sea Res.*, **26A**, 1347-1362.

Peterson M. N. A., N. I. Edgar, C. Von der Borsch, M. B. Cita, S. Gartner, R. Goll and C. Nigrini (1972). Synthesis of initial reports of *Deep-Sea Drilling Project*. II, site 12, 249-303.

Petit J. R., M. Briat and A. Royer (1981). Ice age aerosol content from East Antarctic ice core samples and past wind strength. *Nature*, **293**, 139-194.

Pokras E. M. and A. C. Mix (1985). Eolian evidence for spatial variability of Late Quaternary Climates in Tropical Africa. *Quat. Res.*, **24**, 137-149.

Prospero J. M. (1981). Eolian transport to the World Ocean. In: The Oceanic Lithosphere, C. Emiliani, editor, *The Sea*, **7**, 21, 801-874.

Prospero J. M. and R. T. Nees (1977). Dust concentration in the atmosphere of the equatorial North Atlantic: possible relationship to the Sahelian drought. *Science*, **196**, 1196-1198.

Prospero J. M., E. Bonatti, C. Schubert and T. N. Carlson (1970). Dust in the Caribbean atmosphere traced to an African dust storm. *Earth planet. Sci. Letts.*, **9**, 287.

Pujol C. (1980). Les foraminifères planctoniques de l'Atlantique Nord au Quaternaire. Écologie, stratigraphie, environnement. *Mém. IGBA*, **10**, 1-254.

Rahn K. A. (1986). The chemical composition of the atmospheric aerosol. *Technical Report*, Graduate School of Oceanography, RI-USA, pp. 265.

Rossignol M. and D. Duzer (1979). Late Quaternary pollen and dinoflagellate cysts in marine cores off West Africa. *Meteor Forschergebn.*, **30**, 1-14.

Sarnthein M. and L. Diester-Haass (1977). Eolian-sand turbidites. *J. sedim. Petrology*, **47**, 2, 868-890.

Sarnthein M. and B. Koopmann (1979). Late Quaternary deep-sea record on northwest African dust supply and wind recirculation. In: *Paleo-ecology of Africa*, A. Balmeka, editor, **12**, 239-253.

Sarnthein M., G. Tetzlaff, B. Koopmann, K. Wolter and U. Pflaumann (1981). Glacial and Interglacial wind regimes over the eastern subtropical Atlantic and North West Africa. *Nature*, **293**, 193-196.

Sarnthein M., H. Erlenkeuser and R. Zahn (1982). Termination I: the response of continental climate in the subtropics as recorded in deep-sea sediments. Colloque International CNRS, Bordeaux 22/25-09-81, *Bull. IGBA*, **31**, 393-407.

Savoie D. L. and J. M. Prospero (1977). Aerosol concentration statistics for the Northern Tropical Atlantic. *J. Geophys. Res.*, **82**, 5954-5964.

Tetzlaff G. and K. Wolter (1979). Meteorological patterns and transport of chemical dust from the North African continent. In: *Paleo-Ecology of Africa and surrounding islands*, **13**, 113-128.

Thompson L. G. and E. M. Mosley-Thompson (1981). Micropatticle concentrations linked with climatic changes: evidence from polar ice-cores. *Science*, **212**, 812-814.

Tian R. C. (1984). La sédimentation dans la plaine abyssale du Cap-Vert depuis 18 000 ans. *Mémoire DEA, Université Bordeaux I*, 96 pp.

Veron A., C. E. Lambert, A. Isley, P. Linet and F. Grousset (1987). Evidence of recent lead pollution in deep north-east Atlantic sediments. *Nature*, **326**, 278-281.

Windom H. L. (1969). Atmospheric dust records in permanent snowfields: implication for marine sedimentation. *Geol. Soc. Am. Bull.*, **80**, 761-782.